Speeding up local correlation methods: System-inherent domains

Daniel Kats[1]

Institut für Theoretische Chemie, Universität Stuttgart, Pfaffenwaldring 55, D-70569 Stuttgart, Germany

A new approach to determine local virtual space in correlated calculations is presented. It restricts the virtual space in a pair-specific manner on the basis of a preceding approximate calculation adapting automatically to the locality of the studied problem. The resulting pair system-inherent domains are considerably smaller than the starting domains, without significant loss in the accuracy. Utilization of such domains speeds up integral transformations and evaluations of the residual, and reduces memory requirements. The system-inherent domains are especially suitable in cases which require high accuracy, e.g., in generation of pair-natural orbitals, or for which standard domains are problematic, e.g., excited-state calculations.

I. INTRODUCTION

Wavefunction-based methods have various favorable features, e.g., systematical improvableness, capturing of subtle physical effects, etc. But these features come with a price of evaluation and contraction of high dimensional tensors that occur in the formalism, and the resulting steep scaling of computational resources with the molecular size. Fortunately the dynamical electron correlation is a local phenomenon, and therefore in an appropriately localized basis the tensors are sparse. This represents a basis for various local correlation methods,[1–34] which apply different local approximations to the tensors in order to reduce the computational scaling. The local approximations apply to truncations of the pair list[9,15,35–37] and virtual space restrictions. In this contribution we focus on the latter type of approximation.

There exist several approaches to determine the local virtual basis. One of the first elaborate ways is the Boughton-Pulay procedure[38], which uses information from the Hartree-Fock calculation, i.e., orbitals and partial charges, in order to find important excitation centers in the projected-atomic-orbital (PAO) virtual basis[5,39–41] for a given localized occupied orbital. This procedure was specifically designed for PAO-based methods and is widely used in various implementations.[9–16,42–47] An alternative way is to use information from a correlation method, e.g., a (approximate) second-order perturbation theory, to obtain an optimally compact basis for the higher order treatment. This approach is used in methods based on the orbital-specific virtuals (OSVs)[23–25,48,49] and the pair-natural orbitals (PNOs).[18–22,50–54] It offers a scheme to construct a new virtual basis, which is adapted to recover more correlation energy using smaller number of orbitals. A big advantage of these methods is a smooth approach to the canonical results controlled by a single truncation threshold. The most compact representation of the doubles amplitudes is achieved with the PNO virtual space. However, the integrals and overlap matrices can become large, and an additional overhead of integral transformations and redundant calculations is introduced. The PNO methods often employ PAOs in order to reduce the cost of integral transformations, which triggered fresh demand for optimal PAO pair domains.[22,51–54]

It is possible to use the information from the correlated calculation to define truncations also in the PAO space. However, because of the non-orthogonality of the PAO space a straight-forward application of this type of truncation to the PAO-based methods is problematic. A simple approach of dividing pair-energy contributions according to atomic centers and neglecting all contributions below a certain threshold suffers from the well-known problems of the Mulliken partial charges, i.e., the basis-set (and in this case also starting-domains) dependence and the resulting arbitrariness of small contributions.[24,55] Although it is possible to use orthogonal localized virtual orbitals[56–59] instead of PAOs to circumvent this problem, the PAO space itself has very nice properties, e.g., inexpensive integral transformations as shown in Paper I.[60] An alternative solution is to use a completeness criteria for PAO domains, as was demonstrated with Laplace domains in the context of excited states[17,61–64] where a priori definition of domains using spatial criteria is not appropriate. The resulting procedure corresponds to the OSV procedure without definition of special orbitals.

In this paper we will demonstrate that one can determine the system-inherent domains in PAO space using approximate doubles amplitudes in analogy to OSV and PNO methods. Additionally we will address the problem of ordering PAO-centers which is not trivial because of the non-orthogonality of the PAOs, and we will try to further reduce the domain sizes and the basis set dependency of the domains by using a finer grained PAO space.

II. THEORY

A. Pair and orbital system-inherent domains

The first step in the definition of orbital system-inherent (OSI) or pair system-inherent (PSI) domains is the choice of the approximate amplitudes to represent the molecular system. Here we adopt the usual OSV or PNO practice of using approximate zeroth-iteration local MP2 amplitudes calculated using large starting domains, i.e., amplitudes obtained in pseudo-canonical virtual basis and using only diagonal elements of the occupied Fock matrix in the local basis,[9]

$$\bar{T}^{ij}_{ab} = -\sum_{\bar{a},\bar{b}} W^{ij}_{a\bar{a}} W^{ij}_{b\bar{b}} \frac{\sum_{a',b'} K^{ij}_{a'b'} W^{ij}_{a'\bar{a}} W^{ij}_{b'\bar{b}}}{\epsilon^{ij}_{\bar{a}} + \epsilon^{ij}_{\bar{b}} - f_{ii} - f_{jj}}, \qquad (1)$$

with the approximate amplitudes ($\bar{T}$), pair-specific PAO-to-pseudo-canonical-virtuals transformation matrices (W), two-electron repulsion integrals (K), occupied part of the Fock matrix (f), and virtual-orbital energies in the pseudo-canonical basis (ϵ). Here and in the following i, j, k and a, b, c denote localized occupied orbitals and PAOs, respectively, and $\bar{a}, \bar{b}$ denote the pseudo-canonical virtual orbitals. The pseudo-canonical virtual basis is domain specific, and in order to obtain the W matrices for each pair two matrix-diagonalizations with the pair-domain dimensions have to be performed.[9] It has been shown before that these amplitudes yield reasonable PNOs and OSVs.[22–24,51] However, it is also possible to use doubles amplitudes obtained from a rough Laplace integration,[17] or any other doubles amplitudes.

For OSI domains only approximate doubles amplitudes for diagonal pairs ($\bar{T}^{ii}_{ab}$) are necessary, for PSI domains one needs doubles amplitudes for all pairs ($\bar{T}^{ij}_{ab}$). In the following we will focus on PSI domains, but the formalism is applicable to the OSI domains as well.

Having the amplitudes we are in the position to determine the PSI domains. For that we partition the virtual space onto groups of PAOs, which we call *grains*. Ideally grains should be sensibly small in order to exploit the full potential of the locality in the system, and should be reasonably separated in the real space or energetically. On the other hand, the grains must not be too small, otherwise the domain generation and handling of small blocks in the calculations can become too expensive. On the basis of a certain criterion, discussed below, we rank the PAO grains according to their importance, and add to the domains one after another until a completeness criterion is satisfied.

The system-inherent domains allow for a different blocking of the virtual space than the usual atom-wise graining. This can reduce the size and basis-set dependency of the domain sizes. As an example we have chosen an electronic-subshell-wise graining, i.e., PAO space is grained according to the s, p, d, etc. functions.

As in PNO case the PSI domains can be defined according to energetic or density-matrix criteria. We will stick to the energetic criterion as it also allows for evaluation of approximate energies, which can be used for a domain-error correction (*vide infra*).

First, correlation-energy contribution for a given pair is calculated and divided according to grains,

$$\begin{aligned} e^{ij}_{G} &= \sum_{a\in G}\sum_{b} \frac{1}{2}\left(\tilde{K}^{ij}_{ab}\bar{T}^{ij}_{ab} + \tilde{K}^{ij}_{ba}\bar{T}^{ij}_{ba}\right) \\ \tilde{K}^{ij}_{ab} &= 2K^{ij}_{ab} - K^{ij}_{ba}, \end{aligned} \qquad (2)$$

where G indexes individual grains in the PAO space. Here and in the following an unrestricted summation over virtual indices means that the summation is restricted according to the large starting domains.

Then the grain energies of the pair are sorted in the descending order according to their absolute values, and added up to a certain rough threshold to define starting intermediate domains for the following procedure. In the refinement step the amplitudes are recalculated using the current domains and Eq. (1), and the current pair energy is compared to the full pair energy (which will always have a larger or equal absolute value). If the ratio is below a threshold θ_{PSI} new grains will be added to the domain and the refinement step will be repeated.

A similar procedure has been used before to define Laplace orbital domains for excited states in Ref. 17 with the difference that only OSI domains have been generated, and the approximate amplitudes have been calculated using Laplace transformation. In Ref. 55 a similar idea to define pair domains using approximate amplitudes has been tested. For this the atom-wise pair energy contributions as in Eq. (2) have been calculated and only PAOs on the atomic centers corresponding to large e^{ij}_{G} have been included into pair domain. The conclusion was that the resulting domains have to be rather large for high accuracy, which is probably related to the aforementioned problems of the Mulliken population analysis.

Note that instead of recalculating the amplitudes one can use projection of the full $\bar{T}^{ij}_{ab}$ amplitudes to the smaller domains,

$$\bar{T}^{ij}_{ab}\Big|_{ab\in[ij]_{\text{PSI}}} \approx \sum_{cd} \bar{T}^{ij}_{cd} P^{\mathrm{f}\to[ij]}_{ca} P^{\mathrm{f}\to[ij]}_{db}, \qquad (3)$$

which is approximately two times less expensive, since only one matrix in the current domain has to be diagonalized (the overlap matrix). $\bar{T}^{ij}_{ab}\Big|_{ab\in[ij]_{\text{PSI}}}$ are the approximate doubles amplitudes for the PSI domain of the pair ij, and $\mathbf{P}^{\mathrm{f}\to[ij]}$ is the projector from the full PAO space (or large PAO domain in which $\bar{T}^{ij}_{ab}$ is calculated) to the current $[ij]_{\text{PSI}}$ domain,

$$P^{\mathrm{f}\to[ij]}_{ca} = \sum_{b\in[ij]_{\text{PSI}}} S_{cb} S_{([ij])}{}^{+}_{ba}, \qquad (4)$$

with $\mathbf{S}$ the PAO overlap matrix and $\mathbf{S}_{([ij])}{}^{+}$ the pseudo-inverse of $\mathbf{S}$ in the $[ij]_{\text{PSI}}$ domain[47]. The projection method is applicable also in the situations for which the perturbation theory does not work well, e.g., for systems with multireference character, and can be therefore of interest for the distinguishable cluster method[65–68] and other single-reference methods for strong correlation.[69–77] However, in our tests in sec. III we simply recalculate the amplitudes using Eq. (1).

One can use the approximate amplitudes for a domain-error correction, i.e.,

$$T_{ab}^{ij\mathrm{corr}} = T_{ab}^{ij}\Big|_{ab\in[ij]_{\mathrm{PSI}}} + \bar{T}_{ab}^{ij} - \bar{T}_{ab}^{ij}\Big|_{ab\in[ij]_{\mathrm{PSI}}}, \qquad (5)$$

where T_{ab}^{ij} denote final doubles amplitudes. The corresponding energy correction can be calculated without any additional cost, since the approximate energies are computed anyway during the PSI domain construction procedure.

B. Improved estimate for the grain importance

Although the grain importance can be estimated as described in the previous section, this estimate is not ideal. It is related to partial charges and therefore shares their basis-set (and starting-domains) dependence[24]. Apart from that in a non-orthogonal basis a grain is able to additionally represent energy contributions from other grains, the capability which is completely neglected in the estimate from Eq. (2).

Using an energy intermediate

$$E_{ab}^{ij} = \sum_c \frac{1}{2}\left(\tilde{K}_{ac}^{ij}\bar{T}_{bc}^{ij} + \tilde{K}_{ca}^{ij}\bar{T}_{cb}^{ij}\right), \qquad (6)$$

the estimate from Eq. (2) can be written as

$$e_G^{ij} = \sum_{a\in G} E_{ab}^{ij}\delta_{ab}. \qquad (7)$$

Instead of the delta function one can use projection from the full space to a grain space,

$$\begin{aligned} {}^{\mathrm{c}}e_G^{ij} &= \sum_{dc\in G}\sum_{aa'b} S_{ca'}S_{a'a}^{+}E_{ab}^{ij}S_{bd}S_{(G)}{}_{dc}^{+} \\ &= \sum_{d\in G}\sum_{ab} E_{ab}^{ij}P_{bd}^{\mathrm{f}\to G}P_{da}^{G\to\mathrm{f}}. \qquad (8) \end{aligned}$$

We denote this quantity as the grain *capacity*. It represents a least-square-fitted energy contribution that the grain is capable to capture. Although the last projector in Eq. (8) is not needed as long as G is a subset of the large starting domains, we have inserted it for completeness. Note that a pseudo-inverse of the overlap matrix can be calculated as the square of a corresponding W^{ij} matrix.

Since one is interested not in the total capacity of the grain, but rather in the amount of the energy the given grain can add if included in domain, one should reduce its capacity by the energy contribution which can be covered by the already present grains. This reduction can be easily calculated by projecting the total energy first onto domain space and then projecting it onto the grain space,

$${}^{\mathrm{r}}e_G^{ij} = \sum_{d\in G}\sum_{b}\sum_{ac\in[ij]_{\mathrm{PSI}}} E_{ab}^{ij}P_{bc}^{\mathrm{f}\to[ij]}P_{cd}^{[ij]\to G}P_{da}^{G\to[ij]}. \qquad (9)$$

This capacity reduction is then subtracted from the corresponding full grain capacity ${}^{\mathrm{c}}e_G^{ij}$. The reduced grain capacities ${}^{\mathrm{rc}}e_G^{ij}$ replace the grain energies in the procedure described in sec. II A. Since time for the calculation of reduced grain capacities is negligible compared to the diagonalizations required in the domain construction, and this estimation of the grain importance respects the non-orthogonality of the virtual space, this procedure was used in all test calculations, sec. III.

Finally, since grains usually have different sizes, we scale the reduced grain capacities with the reciprocal grain sizes. This way smaller grains which can contribute the same amount to the energy as larger grains will be included earlier.

As shown for OSVs[23] and PNOs[22] in order to have smooth energy potential surfaces and accurate relative energies it is important to have not only a completeness threshold, but also to include all grains that have energy contributions above some certain threshold. Therefore similarly to Werner et al.[22] additionally to the completeness threshold θ_{PSI} we have introduced a grain-energy threshold θ_{egr}, and if absolute value of the reduced capacity of a grain is larger than the threshold, the grain is included into domain, even if the domain is already complete according to the completeness threshold. Additionally we have introduced a deletion threshold θ_{del} to reduce the size of the domains. If the reduced capacity of a grain is below θ_{del}, then it is not considered for the domain, even if the domain is not complete yet.

The final procedure for PSI-domain construction is summarized as pseudocode in Figure 1. First, integrals K, a pseudocanonical transformation matrix W, amplitudes $\bar{T}$ and a pair energy E^{ij} are calculated using the large starting domain for a given pair ij. Then the scaled capacities for all grains in the large domain are calculated and sorted according to their absolute values. This array is then used to build the intermediate domains using an intermediate completeness criterion. In the main step of the procedure a pseudocanonical transformation matrix and amplitudes are calculated using the current PSI domains, grain energies are recalculated for grains in the PSI domain, and reduced grain capacities are evaluated for the grains outside. The scaled absolute values of the reduced grain capacities are utilized to find the next grain to be added. Finally, the completeness of the PSI

```
Calculate $K^{ij}_{ab}$, $W^{ij}_{a\bar{a}}$, $\bar{T}^{ij}_{ab}$, $E^{ij} = \sum_G e^{ij}_G$ using large starting domains
Calculate $\left({}^{\mathrm{c}}e^{ij}_G / n^{\mathrm{PAO}}_G\right)$ and sort in the descending order of absolute values
do                                                ▷ intermediate domain construction
    Add another grain to the pair domain $[ij]$ according to $\left({}^{\mathrm{c}}e^{ij}_G / n^{\mathrm{PAO}}_G\right)$ array
while $\frac{\sum_{G\in[ij]} |{}^{\mathrm{c}}e^{ij}_G|}{\sum_G |{}^{\mathrm{c}}e^{ij}_G|} < \theta_{\mathrm{Intermediate}}$
do                                                ▷ PSI domain construction
    Calculate $W^{ij}_{a\bar{a}}$, $\bar{T}^{ij}_{ab}$ using the current PSI domain
    Calculate $e^{ij}_G$ for grains in the domain
    Calculate $|{}^{\mathrm{rc}}e^{ij}_G|/n^{\mathrm{PAO}}_G$ for the rest, find max value $\rightarrow G'$
    Set ADDMORE = true
    if $\left(\sum_{G\in[ij]} e^{ij}_G / E^{ij}\right) > \theta_{\mathrm{PSI}}$ then
        ADDMORE = false
    end if
    if $\left(|{}^{\mathrm{rc}}e^{ij}_{G'}|/n^{\mathrm{PAO}}_{G'}\right) > \theta_{\mathrm{egr}}$ then
        ADDMORE = true
    else if $\left(|{}^{\mathrm{rc}}e^{ij}_{G'}|/n^{\mathrm{PAO}}_{G'}\right) < \theta_{\mathrm{del}}$ then
        ADDMORE = false
    end if
    if ADDMORE then
        Add the grain $G'$ to the pair domain $[ij]$
    end if
while ADDMORE
```

FIG. 1. Pseudocode for the PSI-domain construction for a pair ij

domain and the magnitude of the next grain is checked, and either the new grain is added, and the last step is repeated, or the current domain is the final PSI domain for the pair ij.

III. RESULTS

The procedure described in sec. II has been implemented in the development version of MOLPRO[78,79], and the local MP2 (LMP2) equations in the PSI domains are solved using the local integrated tensor framework (LITF)[25]. The PSI-domain generation is completely independent for each orbital pair and can be therefore efficiently parallelized.

The PSI domains have been benchmarked using reactions from Ref. 22 (studied before in Refs. 80–82) with the aug-cc-pVTZ basis (cc-pVTZ for H atoms) and a dye dyad solvent cluster from Ref. 47 (denoted in the following as DA) with the cc-pVTZ basis (492 correlated electrons and 3962 AOs). For calculations in the aug-cc-pVTZ basis the contributions of the most diffuse functions of each angular momentum have been discarded in the Pipek-Mezey localization[83] (the `cpldel=1` option in MOLPRO).

The approximate amplitudes have been calculated as

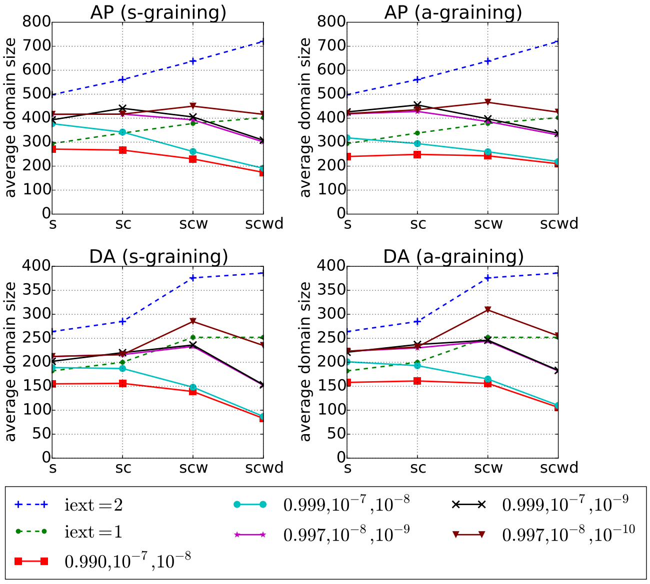

FIG. 2. Average pair-domain sizes for various pair types (s: strong, sc: strong and close, scw: strong, close and weak, scwd: strong, close, weak and distant) for the androstendione precursor (AP) and the dye dyad solvent cluster (DA), and for subshell and atom-wise gaining (s- and a-graining, respectively). The thresholds correspond to θ_{PSI}, θ_{egr}, and θ_{del}, respectively.

the zeroth iteration of the local MP2 using very large domains: Boughton-Pulay domains[38] (threshold 0.985) extended by two shells of neighboring atoms (the `iext=2` option in MOLPRO). It has been shown in Ref. 22 that the local errors of these domains are usually negligible. In the case of reaction III from Ref. 22, which involves a calculation of a transition state, a distance criterion instead of the neighboring criterion was used as suggested by Werner et al.: the Boughton-Pulay domains were extended by atoms which are closer than 6 bohr to the original atoms in the domain (the `rext=6` option in MOLPRO).

Figure 2 shows average pair-domain sizes for various thresholds for the androstendione precursor (the largest molecule from Reaction I, denoted as AP) and the DA system for the subshell- (s-) and atom-wise (a-) graining. The domain sizes are shown for pairs with the inter-orbital distance up to 1 bohr (strong pairs), up to 3 bohr (strong and close pairs), up to 8 bohr (strong, close and weak pairs), and up to 15 bohr (strong, close, weak and distant pairs). Pairs with the inter-orbital distance larger than 15 bohr were neglected in the calculations. Additionally the `iext=2` and `iext=1` domains are shown. One can see that in opposite to the `iext`-domains the size of PSI domains does not increase for pairs with larger inter-orbital distances, and for loose deletion thresholds the average size of domains actually decreases. The subshell-grained domains are usually smaller than the atom-grained ones. Only for loose deletion thresholds the

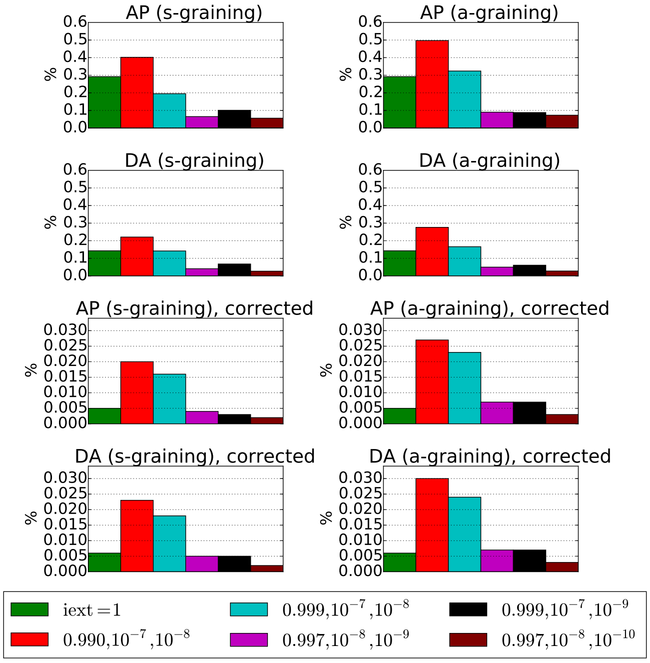

FIG. 3. Relative errors in the pure and corrected correlation energies (in %) compared to iext=2 result for AP (-5.14088 hartree) and DA system (-16.4309 hartree). The thresholds correspond to θ_{PSI}, θ_{egr}, and θ_{del}, respectively.

TABLE I. Timings for the PSI domain construction step ($t_{\mathrm{PSI\ dom}}$), one PAO-LMP2 iteration ($t_{\mathrm{iter.}}$), and the total time for PSI domains and solution of LMP2 equations using algorithm from Paper I[60] (in seconds), as well as peak memory usage in LITF (in megabytes) for AP and DA systems with the atom-wise graining. The calculations have been performed on 10 CPU cores using Intel Xeon E5-2690, 2.8 GHz processor.

θ_{PSI}	iext=2	iext=1	0.990	0.999	0.997	0.999	0.997
θ_{egr}			10^{-7}	10^{-7}	10^{-8}	10^{-7}	10^{-8}
θ_{del}			10^{-8}	10^{-8}	10^{-9}	10^{-9}	10^{-10}
				AP			
$t_{\mathrm{PSI\ dom}}$	0	0	267	279	346	360	477
$t_{\mathrm{iter.}}$	312	76	19	23	47	50	82
$t_{\mathrm{PSI+MP2}}$	3119	758	459	507	819	864	1300
Memory[a]	1663	784	440	474	676	634	921
				DA			
$t_{\mathrm{PSI\ dom}}$	0	0	280	287	383	390	623
$t_{\mathrm{iter.}}$	541	211	42	45	116	118	225
$t_{\mathrm{PSI+MP2}}$	4870	1898	656	695	1431	1453	2645
Memory[a]	6688	5257	3597	3759	4368	4537	5075

[a] Peak memory usage per core. The actual memory requirements are lower.

atom-wise graining yields smaller domains due to the fact that we delete *size-scaled* grains, and therefore the large atom grains are deleted more frequently than the smaller subshell grains (leading to larger errors, *vide infra*). Besides the use of the grain capacity slightly favors smaller grains, i.e., two grains combined will have smaller (or the same) capacity as the sum of individual capacities of the grains.

The corresponding errors in the correlation energies compared to iext=2 results can be found in Figure 3. The zeroth-iteration correction improves results by an order of magnitude. Apparently, the correction is less powerful in correcting small contributions neglected in the case of a loose deletion threshold. It can be seen especially well by comparing uncorrected and corrected results for iext=1 and $\{0.999, 10^{-7}, 10^{-8}\}$ domains. Obviously the effect of the correction will be smaller in the case of coupled-cluster calculations, since the missing parts will be corrected with the zeroth iteration of MP2 only.

All other molecules in the test set show similar trends in domain sizes and errors.[84] Interestingly, with the subshell-wise graining the virtual space can be truncated even for small molecules like HCl: its average domain size is 57 for all tested thresholds versus 64 for full domains.

The timings and peak memory usage for AP and DA systems are given in Table I. The time for PSI domain construction is comparable to one LMP2 iteration with the iext=2 domains, and the LMP2 iteration itself is speeded up by a factor of 3 to 6 without a significant loss of accuracy. The LMP2 iteration time with the most accurate PSI domains considered here is nearly the same as the iteration time with the much less accurate iext=1 domains. The total computational time for solving LMP2 equations (including the PSI domain construction) is also significantly reduced compared to the standard domains. Obviously, memory requirements are also reduced, since the doubles amplitudes are much more compact with the PSI domains. The number of iterations required in the domain-generation procedure is strongly dependent on the threshold for rough intermediate domains. In our calculations we have employed a very loose value for the intermediate-domain threshold (0.6), which can be tighten to 0.8 or 0.9 to speed up the domain construction. One can also use more elaborate techniques, e.g., binary-search algorithm, i.e., adding a fixed number of grains every time and once the completeness condition is satisfied using the binary search to find the optimal number of grains. The scaling of LMP2 equations using the algorithm from Paper I[60] with respect to the pair-domain size is $\mathcal{O}(n_{\mathrm{pdom}}^2 n_{\mathrm{udom}})$, with n_{pdom} pair-domain size, and n_{udom} united-domain size. Therefore the iteration time in Table I scales approximately quadratically with respect to the average pair-domain sizes (since the sizes of united domains vary less). One would gain even more in the local coupled-cluster with doubles calculations, where one has contractions scaling with the fourth power of the pair-domain size.

Deviations in reaction energies from iext=2 results (or rext=6 for Reaction III) for the same choice of thresh-

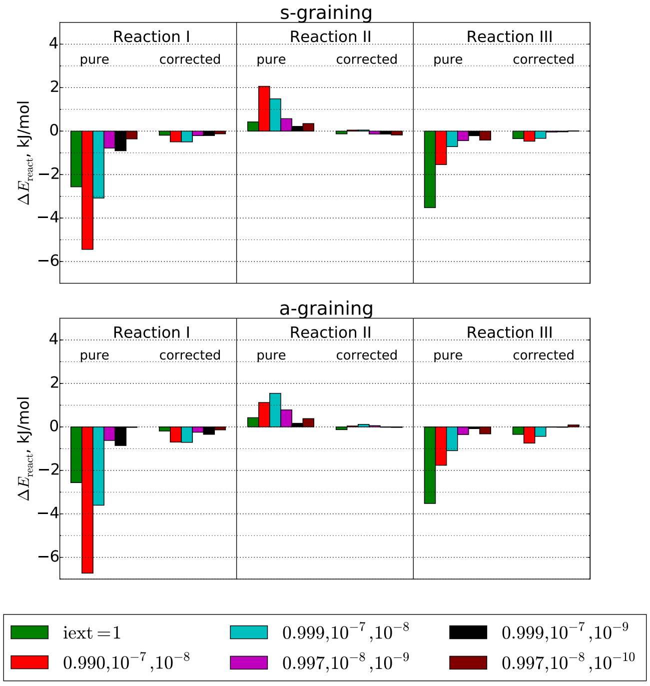

FIG. 4. Deviations in reaction energies for the subshell-wise (top) and atom-wise (bottom) graining compared to iext=2 or rext=6 (for Reaction III) results (in kJ/mol). The thresholds correspond to $\theta_{\rm PSI}$, $\theta_{\rm egr}$, and $\theta_{\rm del}$, respectively.

olds as before are plotted in Figure 4. Apparently, the zeroth-iteration correction works very well even for relative energies: even with the loosest thresholds used here ($\theta_{\rm PSI} = 0.99$, $\theta_{\rm egr} = 10^{-7}$, $\theta_{\rm del} = 10^{-8}$) the corrected reaction energies reach the sub-kilojoule accuracy. As noted in previous studies[22,81,82] the Reaction III involving a transition state calculation is very sensitive to the choice of the large starting domains, cf. Figure 5. The iext=2 domains lead to an error of around 3 kJ/mol for the reaction barrier, and calculations with the rext=5 domains result in an error of around 1 kJ/mol. The average size of the standard domains noticeably increases by going from rext=5 to rext=6 domains. On the other hand changes in the sizes of PSI domains are rather minor, which underlines one of the main advantages of the PSI domains - adaptivity to molecular systems of interest. It is therefore advisable to use as large starting domains as possible and let the PSI domains adapt to the problem afterwords. For example, safer starting domains can be generated using the differential overlap integral,[54] or the much simpler partial-charge overlap criterion introduced in Paper I.[60]

Additionally the basis-set dependence of PSI domains has been investigated using a glycine-dimer molecule. The results can be found in Figure 6. The usual behaviour of the standard domains can be observed: by increasing the basis set the ratio of average pair-domain sizes to the full-domain sizes remains nearly constant.

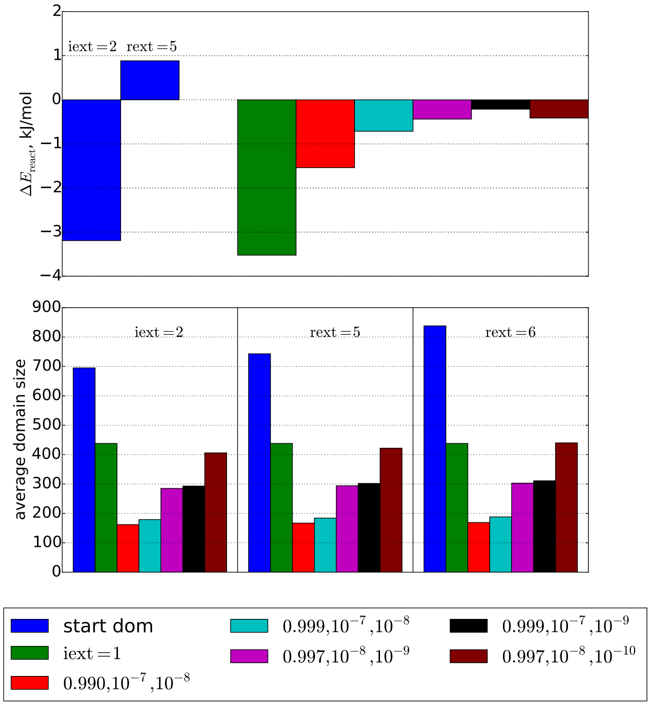

FIG. 5. Top: Deviations in the reaction barrier height for the Reaction III for iext=2, rext=5 and PSI domains (using the subshell-wise graining) compared to rext=6 results (in kJ/mol). Bottom: Average pair-domain sizes from approximate amplitudes calculated using different choices of starting domains (for the transition state system of Reaction III). The thresholds correspond to $\theta_{\rm PSI}$, $\theta_{\rm egr}$, and $\theta_{\rm del}$, respectively.

Contrariwise, the ratio for PSI domains reduces quite fast and is nearly halved by going from aug-cc-pVDZ to aug-cc-pV5Z basis. As expected, this reduction is slightly larger for the subshell-wise graining, although the difference to the atom-wise graining is rather small. The energy accuracy remains nearly constant for the PSI domains, whilst the quality of the results for standard domains noticeably increases.

Summarizing the results, for fast exploratory calculations very loose thresholds (e.g., $\theta_{\rm PSI} = 0.99$, $\theta_{\rm egr} = 10^{-7}$, $\theta_{\rm del} = 10^{-8}$) with the zeroth-iteration correction can be used; for more reasonable domains one should go to a tighter $\theta_{\rm PSI}$ threshold (e.g., $\theta_{\rm PSI} = 0.999$) which results in an accuracy comparable to iext=1 setting; and for highly accurate results even without the correction one should tighten also other thresholds (e.g. $\theta_{\rm PSI} = 0.997$, $\theta_{\rm egr} = 10^{-8}$, $\theta_{\rm del} = 10^{-9}$ or even $\theta_{\rm del} = 10^{-10}$, which is close to the set of thresholds recommended for PNO calculations in Ref. 22).

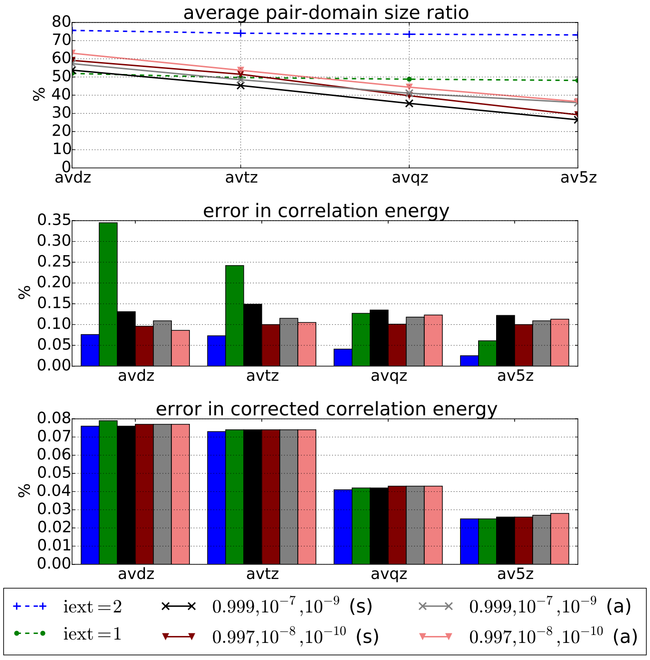

FIG. 6. Basis-set dependence of the iext and PSI domains (with the subshell-wise (s) and atom-wise (a) graining), i.e., ratios of the average pair-domain sizes to the full-domain sizes (top) and the corresponding relative errors in the correlation energies compared to canonical results without (middle) and with (bottom) the zeroth-iteration correction for a glycine-dimer molecule. The thresholds correspond to θ_{PSI}, θ_{egr}, and θ_{del}, respectively.

IV. CONCLUSION

The PSI domains represent an analogue of PNOs in the PAO space (or any other choice of the virtual space). They share some advantages with PNOs, e.g., adaptivity and systematical improvability, but do not require a new set of orbitals. In contrast to the standard domains and similar to PNOs the size of PSI domains does not increase by going to more distant pairs, and has much lower basis-set dependence. However, still 3 to 5 times more PAOs than PNOs per pair are needed for the same accuracy. The PAO integral transformations can be made quite inexpensive (by using semi-direct integral transformations to the PAO space[60]), and algorithms can take advantage of using united domains,[60,85] which makes PAOs interesting not only for PAO-based local methods, but also as an intermediate step in the PNO construction,[22,51–54] and the PSI domains would allow larger (i.e., safer) starting domains and speed up integral transformations. This will be investigated in a forthcoming publication.

The subshell-wise graining turned out to be less important, since the atom-wise grained domains are not much worse than the subshell-wise domains. However, if one wants to squeeze out all the potential of the PSI domains, one should use a subatomic graining. One can also try alternative grainings, e.g., according to diffuseness of the functions, etc.

Further improvements in the PSI-domain generation are feasible. One can use more sophisticated heuristic to sort the grains, and one can a posteriori try to eliminate grains from the domains which turn out to be not important in the final domains. In order to speed up the domain generation one can add a fixed amount of grains to the domains in each step, and use a binary search algorithm to find the minimal amount of grains needed. For an efficient code with a subshell-wise graining one has to combine grains which usually occur together in order to increase the block size (it is especially important for the local integrated tensor framework[25], which heavily relies on reasonably sized blocks in the orbital spaces). And as noted in sec. II A one can use projection of amplitudes from large domains instead of recalculating them in the domain generation.

The PSI domains can be used in various local correlation methods. As mentioned already, one can use the PSI domains in a PNO generation in order to speed up integral transformations in the PNO-based methods, which usually constitute the bottleneck of the calculation. But the PSI domains can be also important in cases where one has to perform multiple integral transformations, e.g., excited states with adaptive domains[17,61–64] and orbital-optimized methods,[66,86–88] or for which standard domains can fail, e.g., excited and transition states, and strongly-correlated systems.[65,73] Combined with techniques from Paper I the PSI domains can considerably speed up local correlation methods.

ACKNOWLEDGMENTS

The author is grateful to D. Usvyat and H.-J. Werner for helpful discussions. Financial support from ERC (Advanced Grant ASES 320723) is acknowledged.

[1] R. Ahlrichs and W. Kutzelnigg, J. Chem. Phys. **48**, 1819 (1968).
[2] W. Kutzelnigg, in *Localization and Delocalization in Quantum Chemistry*, edited by O. Chalvet et al. (D. Deidel, Dordrecht, 1975) p. 143.
[3] G. Stollhoff and P. Fulde, J. Chem. Phys. **73**, 4548 (1980).
[4] W. D. Laidig, G. D. Purvis III, and R. J. Bartlett, Chem. Phys. Lett. **97**, 209 (1983).
[5] P. Pulay, Chem. Phys. Lett. **100**, 151 (1983).
[6] S. Saebø and P. Pulay, Annu. Rev. Phys. Chem. **44**, 213 (1993).
[7] P. Y. Ayala and G. E. Scuseria, J. Chem. Phys. **110**, 3660 (1999).
[8] P. E. Maslen and M. Head-Gordon, J. Chem. Phys. **109**, 7093 (1998).
[9] C. Hampel and H.-J. Werner, J. Chem. Phys. **104**, 6286 (1996).
[10] M. Schütz and H.-J. Werner, Chem. Phys. Lett. **318**, 370 (2000).
[11] M. Schütz, J. Chem. Phys. **113**, 9986 (2000).
[12] M. Schütz, J. Chem. Phys. **116**, 8772 (2002).
[13] H.-J. Werner, F. R. Manby, and P. J. Knowles, J. Chem. Phys. **118**, 8149 (2003).
[14] M. Schütz and F. R. Manby, Phys. Chem. Chem. Phys. **5**, 3349 (2003).

[15] H.-J. Werner and M. Schütz, J. Chem. Phys. **135**, 144116 (2011).

[16] T. Korona, D. Kats, M. Schütz, T. B. Adler, Y. Liu, and H.-J. Werner, in *Linear-Scaling Techniques in Computational Chemistry and Physics*, edited by R. Zalesny, M. G. Papadopoulos, P. G. Mezey, and J. Leszczynski (Springer Netherlands, Dordrecht, 2011) p. 345.

[17] D. Kats and M. Schütz, J. Chem. Phys. **131**, 124117 (2009).

[18] W. Meyer, Int. J. Quantum Chem. Symp. **5**, 341 (1971).

[19] F. Neese, F. Wennmohs, and A. Hansen, J. Chem. Phys. **130**, 114108 (2009).

[20] F. Neese, A. Hansen, and D. G. Liakos, J. Chem. Phys. **131**, 064103 (2009).

[21] C. Hättig, D. P. Tew, and B. Helmich, J. Chem. Phys. **136**, 204105 (2012).

[22] H.-J. Werner, G. Knizia, C. Krause, M. Schwilk, and M. Dornbach, J. Chem. Theory Comput. **11**, 484 (2015).

[23] J. Yang, Y. Kurashige, F. R. Manby, and G. K. L. Chan, J. Chem. Phys. **134**, 044123 (2011).

[24] J. Yang, G. K. L. Chan, F. R. Manby, M. Schütz, and H.-J. Werner, J. Chem. Phys. **136**, 144105 (2012).

[25] D. Kats and F. R. Manby, J. Chem. Phys. **138**, 144101 (2013).

[26] W. Förner, J. Ladik, P. Otto, and J. Čížek, Chem. Phys. **97**, 251 (1985).

[27] H. Stoll, Chem. Phys. Lett. **191**, 548 (1992).

[28] J. Friedrich, M. Hanrath, and M. Dolg, J. Chem. Phys. **126**, 154110 (2007).

[29] S. Li, J. Ma, and Y. Jiang, J. Comput. Chem. **23**, 237 (2002).

[30] W. Li, P. Piecuch, J. R. Gour, and S. Li, J. Chem. Phys. **131**, 114109 (2009).

[31] W. Li, Y. Guo, and S. Li, Phys. Chem. Chem. Phys. **14**, 7854 (2012).

[32] M. Ziółkowski, B. Jansík, T. Kjærgaard, and P. Jørgensen, J. Chem. Phys. **133**, 014107 (2010).

[33] I.-M. Høyvik, K. Kristensen, B. Jansik, and P. Jørgensen, J. Chem. Phys. **136**, 014105 (2012).

[34] Z. Rolik and M. Kállay, J. Chem. Phys. **135**, 104111 (2011).

[35] O. Masur, D. Usvyat, and M. Schütz, J. Chem. Phys. **139**, 164116 (2013).

[36] M. Schütz, O. Masur, and D. Usvyat, J. Chem. Phys. **140**, 244107 (2014).

[37] M. Schwilk, D. Usvyat, and H.-J. Werner, J. Chem. Phys. **142**, 121102 (2015).

[38] J. W. Boughton and P. Pulay, J. Comput. Chem. **14**, 736 (1993).

[39] S. Saebø and P. Pulay, Chem. Phys. Lett. **113**, 13 (1985).

[40] S. Saebø and P. Pulay, J. Chem. Phys. **86**, 914 (1987).

[41] S. Saebø and P. Pulay, J. Chem. Phys. **88**, 1884 (1988).

[42] T. D. Crawford and R. A. King, Chem. Phys. Lett. **366**, 611 (2002).

[43] T. Korona and H.-J. Werner, J. Chem. Phys. **118**, 3006 (2003).

[44] L. Maschio, D. Usvyat, F. R. Manby, S. Casassa, C. Pisani, and M. Schütz, Phys. Rev. B **76**, 075101 (2007).

[45] D. Kats, T. Korona, and M. Schütz, J. Chem. Phys. **125**, 104106 (2006).

[46] D. Kats, T. Korona, and M. Schütz, J. Chem. Phys. **127**, 064107 (2007).

[47] D. Kats, D. Usvyat, and M. Schütz, Phys. Chem. Chem. Phys. **10**, 3430 (2008).

[48] M. Schütz, J. Yang, G. K.-L. Chan, F. R. Manby, and H.-J. Werner, J. Chem. Phys. **138**, 054109 (2013).

[49] D. Usvyat, L. Maschio, and M. Schütz, J. Chem. Phys. **143**, 102805 (2015).

[50] B. Helmich and C. Hättig, Comp. Theor. Chem. **1040-1041**, 35 (2014).

[51] C. Riplinger and F. Neese, J. Chem. Phys. **138**, 034106 (2013).

[52] C. Riplinger, B. Sandhoefer, A. Hansen, and F. Neese, J. Chem. Phys. **139**, 134101 (2013).

[53] Q. Ma and H.-J. Werner, J. Chem. Theory Comput. **11**, 5291 (2015).

[54] C. Riplinger, P. Pinski, U. Becker, E. F. Valeev, and F. Neese, J. Chem. Phys. **144**, 024109 (2016).

[55] H.-J. Werner and K. Pflüger, Ann. Reports in Comput. Chem **2**, 53 (2006).

[56] J. E. Subotnik, A. D. Dutoi, and M. Head-Gordon, J. Chem. Phys. **123**, 114108 (2005).

[57] J. Subotnik, A. Sodt, and M. Head-Gordon, J. Chem. Phys. **125**, 074116 (2006).

[58] T. S. Chwee and E. A. Carter, J. Chem. Theory Comput. **7**, 103 (2011).

[59] I.-M. Høyvik and P. Jørgensen, Chem. Rev. **116**, 3306 (2016).

[60] D. Kats, J. Chem. Phys. **141**, 244101 (2014).

[61] D. Kats and M. Schütz, Z. Phys. Chem. **224**, 601 (2010).

[62] K. Freundorfer, D. Kats, T. Korona, and M. Schütz, J. Chem. Phys. **133**, 244110 (2010).

[63] K. Ledermüller, D. Kats, and M. Schütz, J. Chem. Phys. **139**, 084111 (2013).

[64] K. Ledermüller and M. Schütz, J. Chem. Phys. **140**, 164113 (2014).

[65] D. Kats and F. R. Manby, J. Chem. Phys. **139**, 021102 (2013).

[66] D. Kats, J. Chem. Phys. **141**, 061101 (2014).

[67] D. Kats, D. Kreplin, H.-J. Werner, and F. R. Manby, J. Chem. Phys. **142**, 064111 (2015).

[68] D. Kats, J. Chem. Phys. **144**, 044102 (2016).

[69] J. Paldus, J. Čížek, and M. Takahashi, Phys. Rev. A **30**, 2193 (1984).

[70] P. Piecuch and J. Paldus, Int. J. Quantum Chem. **40**, 9 (1991).

[71] P. Piecuch, R. Tobola, and J. Paldus, Phys. Rev. A **54**, 1210 (1996).

[72] K. Kowalski and P. Piecuch, J. Chem. Phys. **113**, 18 (2000).

[73] J. B. Robinson and P. J. Knowles, J. Chem. Phys. **135**, 044113 (2011).

[74] D. W. Small and M. Head-Gordon, J. Chem. Phys. **137**, 114103 (2012).

[75] T. Stein, T. M. Henderson, and G. E. Scuseria, J. Chem. Phys. **140**, 214113 (2014).

[76] K. Boguslawski, P. Tecmer, P. A. Limacher, P. A. Johnson, P. W. Ayers, P. Bultinck, S. D. Baerdemacker, and D. V. Neck, J. Chem. Phys. **140**, 214114 (2014).

[77] I. W. Bulik, T. M. Henderson, and G. E. Scuseria, J. Chem. Theory Comput. **11**, 3171 (2015).

[78] H.-J. Werner, P. J. Knowles, G. Knizia, F. R. Manby, M. Schütz, P. Celani, W. Györffy, D. Kats, T. Korona, R. Lindh, A. Mitrushenkov, G. Rauhut, K. R. Shamasundar, T. B. Adler, R. D. Amos, A. Bernhardsson, A. Berning, D. L. Cooper, M. J. O. Deegan, A. J. Dobbyn, F. Eckert, E. Goll, C. Hampel, A. Hesselmann, G. Hetzer, T. Hrenar, G. Jansen, C. Köppl, Y. Liu, A. W. Lloyd, R. A. Mata, A. J. May, S. J. McNicholas, W. Meyer, M. E. Mura, A. Nicklass, D. P. O'Neill, P. Palmieri, D. Peng, K. Pflüger, R. Pitzer, M. Reiher, T. Shiozaki, H. Stoll, A. J. Stone, R. Tarroni, T. Thorsteinsson, and M. Wang, "Molpro, version 2015.1, a package of ab initio programs," (2015), see http://www.molpro.net.

[79] H.-J. Werner, P. J. Knowles, G. Knizia, F. R. Manby, and M. Schütz, WIREs Comput Mol Sci **2**, 242 (2012).

[80] T. B. Adler and H.-J. Werner, J. Chem. Phys. **135**, 144117 (2011).

[81] F. Claeyssens, J. N. Harvey, F. R. Manby, R. A. Mata, A. J. Mulholland, K. E. Ranaghan, M. Schütz, S. Thiel, W. Thiel, and H.-J. Werner, Angew. Chem. **118**, 7010 (2006).

[82] R. A. Mata, H.-J. Werner, S. Thiel, and W. Thiel, J. Chem. Phys. **128**, 025104 (2008).

[83] J. Pipek and P. G. Mezey, J. Chem. Phys. **90**, 4916 (1989).

[84] See Supplementary Material Document No. for the average domain sizes and the corresponding accuracies. For information on Supplementary Material, see http://www.aip.org/pubservs/epaps.html.

[85] M. Schütz, G. Hetzer, and H.-J. Werner, J. Chem. Phys. **111**, 5691 (1999).

[86] G. E. Scuseria and H. F. Schaefer III, Chem. Phys. Lett. **142**, 354 (1987).

[87] C. Kollmar and A. Heßelmann, Theor. Chem. Acc. **127**, 311

(2010).

[88] U. Bozkaya, J. M. Turney, Y. Yamaguchi, H. F. Schaefer, and C. D. Sherrill, J. Chem. Phys. **135**, 104103 (2011).